Thermal Evolution of an Early Magma Ocean

Jodi Gaeman
May 1, 2009
Advisor: Dr. Saswata Hier-Majumder
Final Draft
GEOL394H

Abstract

Planetary magma oceans exist in many forms throughout the solar system. Their thermal evolution, influenced by various forms of heating and cooling, is intricately linked to their crystallization, and thus their internal structural evolution. The connection between these parameters can be illustrated in many cases, including the evolution of a terrestrial basal magma ocean hypothesized to have formed early during Earth's evolution. Several researchers have begun modeling the evolution of a basal magma ocean with respect to these parameters. One recent model illustrated the thermal evolution of the magma ocean as derived from a linear crystallization model. As crystallization within the mantle occurs nonlinearly, this study shows the nonlinear relation between increasing crystal fraction and decreasing temperature and its influence on the existence of magma oceans. Within this study, we have formulated a model coupling the thermal evolution of a magma ocean with the evolution of its interior and the thermal evolution of an overlying mantle. In doing so, our results show significant differences between thermal evolution models produced from both linear and nonlinear crystallization models. It is our intent to extend this study to incorporate a thermal evolution model formulated for the cryomagma ocean found within the interior of Neptune's icy satellite, Triton. Marring Triton's surface is a series of unique ridges formed by unknown processes. The satellite's dynamic orbital history, which caused an increase in internal heating through tidal dissipation, may provide a possible explanation for these ridges. A study of the satellite's thermal evolution may determine the likeliness of internal processes contributing to the geologic activity as opposed to external stresses. Within this study, we have begun to examine the thermal structure of Triton's interior. Ultimately, we will adapt our existing two layer basal magma ocean model to a four layer icy satellite model incorporating tidal dissipation to further investigate the influence of nonlinear crystallization models on the thermal evolution of a planetary body's subsurface ocean.

Table of Contents

List of Figures

1. Crystallizing Terrestrial Basal Magma Ocean

Introduction

As the Earth coalesced 4.5 billion years ago, the heat associated with the accretionary process was substantial enough to allow for partial melting throughout the entire planet. In combination with early greenhouse heating from a primitive atmosphere, impact heating from collisions, and radiogenic heating from the Earth's interior, an early global magma ocean is hypothesized to have formed during the earliest stages of the Earth's evolution (Solomatov and Stevenson, 1993b). Excessive early heating contributed to an initially high temperature, with a correspondingly low viscosity, within the magma ocean - ideal conditions for the "hard" turbulent convective regime characteristic of the early Earth. "Hard" turbulent convective regimes, in contrast to "soft" turbulent convective regimes, typically have large-scale circulation patterns resulting from the turbulence of the system, unlike other forms of convection. This results from the low viscosity values, which are typically on the order of 10^{-1} Pa s (Solomatov, 2000).

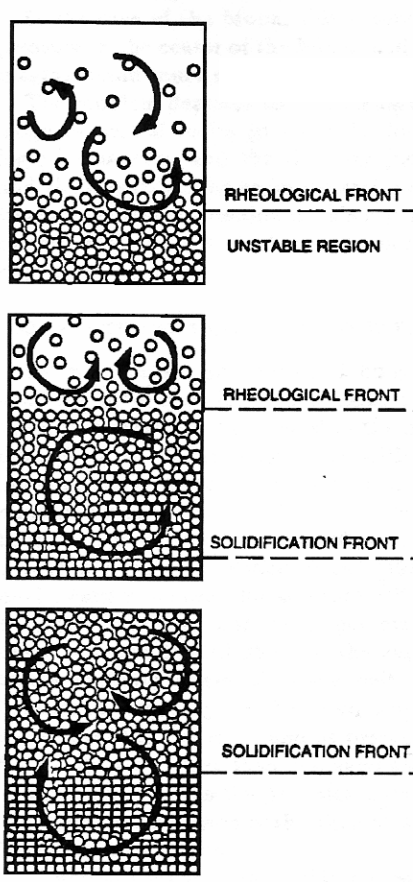

Figure 1: **Magma Ocean Crystallization** – The topmost figure shows the beginning of the rheological transition. Crystals begin settling out towards the bottom of the magma ocean. The middle image shows the beginning of the solidification front. The bottom-most image shows the onset of solid state convection as the solidification front propagates towards the surface. Figure from Scott and Kohlstedt (2006).

As the Earth began to cool, the magma ocean began to crystallize, but maintained the relatively low viscosity values, and thus the "hard" turbulent convective regime, allowing crystals to remain in suspension within the magma ocean, rather than settling out of the system. As the crystal fraction within the magma ocean reached a critical value of approximately 60%, however, a rheological transition occurred. This rheological transition is depicted in Figure 1. At this critical crystal fraction, the viscosity of the system would have jumped several orders of magnitude, from ~10^{-1} to ~10^{16} Pa s, allowing a new convective regime to take over the system, with the previously formed crystals settling towards the bottom of the magma ocean. This designates the rheological front, which then propagated towards the surface of the Earth in a relatively short period, likely about 10^3-10^4 yrs, though there is some variation in this estimate. As crystallization continued, a solidification front followed the rheological front from the base of the magma ocean to the surface, solidifying the mantle, and allowing solid-state convection to become the dominant form of convection within the mantle thereafter (Solomatov and Stevenson, 1993a).

It is unclear how the thermal evolution of the mantle would appear during this time of crystallization from a magma ocean state. Several researchers have put forth various models describing the thermal history of the Earth that may pertain to this period. Schubert et al. (2001) formulated one such thermal evolution model based on a simplified single layer model of the Earth, excluding any interaction

with the core. Derived from the general heat equation, the model mainly considers convection, secular cooling, and radiogenic heating within the mantle. As would be expected for a crystallizing mantle, the model depicts the system starting with a high initial temperature, but then undergoing a rapid decrease in temperature over a 200-300 Myr period, before switching to a more gradual decline. The 200-300 Myr period showing a rapid decline in temperature is perhaps the most interesting part of the plot, as it represents a period of rapid convection within the Earth that ultimately allows the planet to resume a more stable thermal regime (Schubert et al., 2001).

Labrosse et al. proposed another thermal evolution model that relies on a coupled core-mantle system, which is similar to what one would expect when considering the thermal evolution of the Earth. The thermal evolution model is derived from the heat equation, just as in the case of the model from Schubert et al., but also is based on a linearized phase diagram relating the mass fraction of a solid solution MgO - FeO system to the liquidus temperature of the system. Rather than applying this model to a global magma ocean, the authors mainly focus on crystallizing a basal magma ocean. Thus, in addition to solving for thermal history, evolution of the thickness of the magma ocean is parameterized, as well (Labrosse et al., 2007).

As the thermal history model produced by Labrosse et al. (2007) is dependent on the variation of temperature with mass fraction, it is necessary to consider the type of relationship between these two parameters. Labrosse et al. (2007) rely on a linearized crystallization model in which the crystal fraction increases linearly with a decrease in temperature. Laboratory experiments, however, suggest that crystallization within the mantle occurs in a nonlinear manner. A more recent parameterization formulated by Katz et al. (2003) illustrates such a nonlinear relationship. My work focuses on quantifying the result of such a nonlinear crystallization model in the thermal evolution of a magma ocean.

Research Objectives

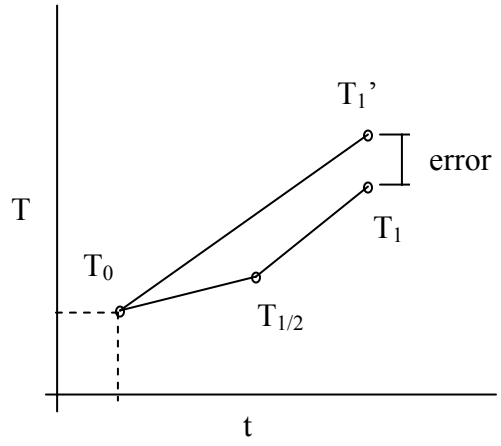

Figure 2 : Error Approximation - This figure illustrates an example of adaptive time stepping for a Temperature v. time model. From initial point T_0, the RK4 algorithm will compute the next T value for a given time step. Adaptive time stepping algorithms can then be used to adjust this time step based on a computed error.

The goal of this project is to determine whether a linearized melting model can be used to approximate the thermal evolution of a mantle from a magma ocean state. It is expected that the thermal histories reproduced by both linear and nonlinear melting models will be distinct. Therefore, I hypothesize that nonlinear melting models will be necessary for thermal evolution approximations, as linearized melting models will be insufficient.

My hypothesis can be falsified by using both crystallization models to solve the thermal evolution equation. The crystallization models are incorporated into an equation describing the evolution of the thickness of the melt layer. Therefore, they will directly influence the thickness of the evolving magma ocean as it undergoes cooling. Analysis of these models will serve to verify or falsify my hypothesis.

Experiment Design

Ultimately, the main goal of this project was to create a new thermal evolution model. The main variables included: temperature and thickness of the magma ocean, which were the unknowns; viscosity and melt fraction, which were the parameters used for varying the system; and time, which was the independent variable.

As this project involved analyzing and formulating new thermal evolution models based on mantle melting parameterizations, the majority of calculations were made using computer programming techniques. In particular, programming and codes relevant to this project have been built using Fortran 90. Visualizations of these models, consisting mainly of various graphs and plots, have been performed with the help of SciLab and MATLAB.

Determination of unknown variables required numerical analysis. Though there are many analytical methods to select from, 4th order Runge-Kutta (RK) approximations are more efficient than other methods. 4th order RK approximations, therefore, were the only analytical technique required for this project. However, in some cases, coupled 4th order RK approximations were required as the need to solve for multiple unknowns using systems of ordinary differential equations arose. A generic algorithm of the 4th order RK equations may be seen below:

$$
\begin{aligned}
k_1 &= F\left(x_n, y_n\right) \\
k_2 &= F\left(x_n + \frac{h}{2}, y_n + h\frac{k_1}{2}\right) \\
k_3 &= F\left(x_n + \frac{h}{2}, y_n + h\frac{k_2}{2}\right) \\
k_4 &= F\left(x_n + h, y_n + hk_3\right) \\
y_{n+1} &= y_n + \frac{h}{6}\left(k_1 + 2k_2 + 2k_3 + k_4\right)
\end{aligned}
\qquad \text{Eq. 1}
$$

Within this approximation, one assumes F is a function varying with independent variable x and dependent variable y. The variable h is considered a time step, while n designates a given location in an array of data (Press et al., 1992). The variables k_1, k_2, k_3, and k_4 serve as constraints from which the next data point may be solved. As all data has been calculated using 4th order RK approximations, error has been approximated by adaptive time stepping procedures. These procedures allow for the length of each step to be adjusted and controlled. This prevents numerical errors from exceeding a preset value. Figure 2 illustrates an example of how adaptive time-stepping procedures may be used. From initial point T_0, RK4 will first calculate point T_1', the next data point in the series, relying on time-step dt, the change of time suggested within the code. RK4 will then compute $T_{1/2}$ and T_1, as determined by ½ of the time step dt. $T_{1/2}$ and T_1 are two separate computations. T_1 will likely differ from T_1' by some amount, which is the calculated error. If this error exceeds a prescribed preset error value, then the time-step can be adjusted as necessary.

Before a new thermal evolution model could be devised, it was necessary to analyze the pre-existing thermal evolution models to determine how each was derived. It was also necessary to be aware of the variables, parameters, and constants incorporated into each model as different models rely on different data as a consequence of differing derivations. In particular, Schubert et al. and Labrosse et al. models were the focus for this analysis. Each of these models needed to be derived and reproduced. Both of these models were originally derived from the heat equation

$$Mc\left(\frac{\mathrm{d}T}{\mathrm{dt}}\right) = MH - Aq \qquad \text{Eq. 2,}$$

where M is mass of the mantle, c is the specific heat of the mantle, T is the average temperature over the mantle, t is time, H is radiogenic heating, A is mantle surface area, and q is heat flux. Likewise, it was also necessary to analyze the pre-existing melting models. The relationship between melt fraction and temperature needed to be assessed for both the linear and nonlinear melting models as this was the main distinction when analyzing thermal evolution.

The next step for this project was to derive new equations for coupled core-mantle interaction. This allowed for a new thermal evolution model, which could be related to the crystallizing magma ocean. The nonlinear melting model data was input for the thermal evolution model and solved numerically using the coupled 4th order RK equations derived for the particular model. The data and corresponding plots created were then used to determine whether linear melting data was sufficient for analyzing the thermal evolution of the early earth.

Governing Equations

Simplified Thermal History Model

Schubert et al.'s parameterized convection model was derived from the heat equation, Eq. 2. As the model excludes any interference from the core, the authors only take into account radiogenic heating, convection, and secular cooling. To better understand the authors' proposed model, Eq. 2 was used to derive the final equations necessary for numerical analysis. The new equation for the single layer model became

$$\left(\frac{\mathrm{d}T}{\mathrm{dt}}\right) = \frac{H_0}{c}\mathrm{e}^{-\lambda t} - \frac{Ak}{Mcd}\left(\frac{\alpha g d^3}{\upsilon_0 Ra_{cr}\kappa}\right)^{\beta}\left(T - T_s\right)^{1+\beta}\mathrm{e}^{\frac{-\beta A_0}{T}} \qquad \text{Eq. 3.}$$

Temperature was numerically solved for using 4th order RK approximations, with time acting as the parameter incrementing the system. In addition to solving for temperature variation, viscosity has been solved for as well to illustrate its dependence on temperature. The derived viscosity equation is

$$\upsilon = \upsilon_0\,\mathrm{e}^{\frac{A_0}{T}} \qquad \text{Eq. 4,}$$

where ν is viscosity, T is temperature.

Thermal Evolution and Melt Layer Evolution from Linearized Phase Diagram

Labrosse et al.'s thermal evolution model based on a linearized phase diagram, shown in Figure 3, is calculated from two equations: the first resulting from the heat equation (Eq. 2), and the second being a relationship between mass fraction and temperature as determined by their phase diagram. The first derived equation is

$$\frac{\mathrm{d}T_L}{\mathrm{dt}} = \frac{1}{M_m C_{pm} + M_c C_{pc}}\left[\frac{-4\pi a^2 k\left(T_L - T_M\right)}{\delta} + H(t) - 4\pi a^2 \rho \Delta S T_L \frac{\mathrm{d}a}{\mathrm{dt}}\right] \qquad \text{Eq. 5,}$$

where T_L is liquidus temperature, T_M is temperature above the solid mantle boundary layer, a is the melt layer radius, M_m is mass of the melt layer, M_c is mass of the core, C_{pm} is specific heat of the melt layer, C_{pc} is specific heat of the core, ρ is the density, k is the thermal conductivity, δ is

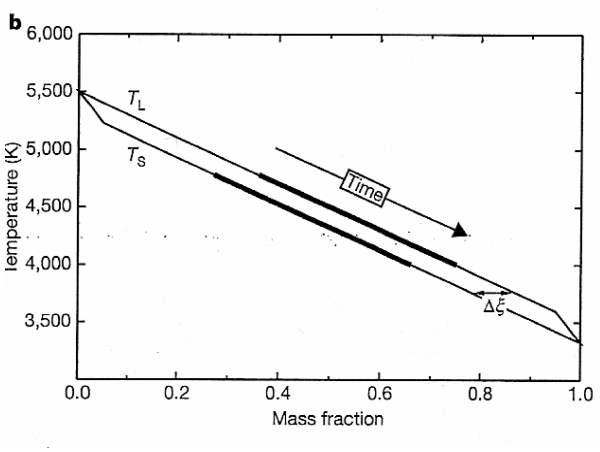

Figure 3: **Linearized Phase Diagram** - from Labrosse et al. (2007)
Figure shows variation of Temperature with Mass fraction of a solid solution (FeO-MgO) system.

the thickness of mantle boundary layer, and ΔS is the specific entropy.

The equation takes into account radiogenic heating, convection, and secular cooling, just as the Schubert et al. model does. In this case, however, because the authors are solving for the thermal evolution of a basal magma ocean with an evolving thickness, a second variable, melt layer radius a, is introduced. As this variable is unknown, a second equation is needed to solve for the system. From the authors' linearized phase diagram, the second derived equation becomes:

$$\frac{\mathrm{d}a}{\mathrm{d}t} = \frac{a^3 - b^3}{3a^2\Delta\xi\left(T_A - T_B\right)}\frac{\mathrm{d}T_L}{\mathrm{d}t} \quad \text{Eq. 6.}$$

By coupling these two equations, it would ideally be possible to solve for the thermal evolution of the basal magma ocean. However, many of the values incorporated in this equation are relatively large, which can cause complications with computer processing. To eliminate these complications, these equations were nondimensionalized within the Fortran codes. As a result of nondimensionalization, Eq. 5 and Eq. 6 became:

$$\frac{\mathrm{d}T_L}{\mathrm{d}t} = Aa^2\left(T_L - \frac{T_M}{T_0}\right) + Ba^2T_L\frac{\mathrm{d}a}{\mathrm{d}t} + C\,\mathrm{e}^{-\lambda t_0 t} \qquad \text{Eq. 7,}$$

where:

$$A = \frac{-4\pi a_0^2 k t_0}{\delta\left(M_m C_{pm} + M_c C_{pc}\right)}$$

$$B = \frac{-4\pi a_0^2 \rho\Delta S T_0}{M_m C_{pm} + M_c C_{pc}}$$

$$C = \frac{Ht_0}{T_0\left(M_m C_{pm} + M_c C_{pc}\right)}$$

$$\frac{\mathrm{d}a}{\mathrm{d}t} = D\left(a - \frac{\left(b/a_0^2\right)^3}{a^2}\right)\frac{\mathrm{d}T_L}{\mathrm{d}t} \qquad \text{Eq. 8,}$$

where:

$$D = \frac{T_0}{3\left(T_A - T_B\right)\Delta\xi}$$

Thermal Evolution and Melt Layer Evolution from Nonlinear Crystallization Model

After completing thermal evolution models based on a linearized phase diagram depicting melting and crystallization within the magma ocean, the next step was to develop a model of thermal evolution based on nonlinear crystallization within the mantle. For this project, nonlinear mantle crystallization data was applied based on Katz et al.'s parameterized melting models. To achieve this, it was necessary to have two equations, coupling dT_L/dt with da/dt. For this model, we could reuse Eq. 5 for dT_L/dt (and Eq. 7). A new equation, however, had to be derived for da/dt. First, we derived a relationship between melt fraction F and melt layer radius a.

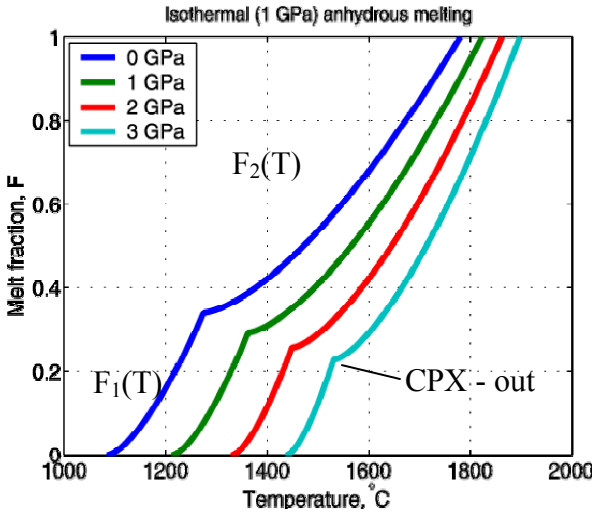

Figure 4: Nonlinear Melt Fraction - This plot is showing the nonlinear relationship between melt fraction and temperature, as formulated by Katz et al. The kinks represent the points at which cpx is exhausted from the melt. F_1 in Eq. 10 is derived from the equation describing the graph at T<T(kink). F_2 in Eq. 10 is derived from the equation describing the graph at T>T(kink). Plot taken from Katz et al. (2003).

$$F = \frac{a^3 - b^3}{a_0^3 - b^3} \qquad \text{Eq. 9,}$$

where b is the radius of the core, and a_0 is the crystallized portion of the magma ocean.

From Katz et al., two relationships have been derived between melt fraction and temperature: the first pertaining to the melt before clinopyroxene (cpx) has been exhausted, and the second pertaining to the melt after cpx exhaustion. Figure 4 depicts this relationship. An equation for melt fraction as a function of temperature was derived from these, which can be applied to the thermal evolution model.

$$F = \mathrm{g}_1(T_c - T_L)\mathrm{F}_1(T_L) + \mathrm{g}_2(T_L - T_c)\mathrm{F}_2(T_L) \qquad \text{Eq.10,}$$

where the function g(x) = 0 if x < 0 or g(x) = 1 if x>0. However, the values used by Katz et al. for determining F_1 and F_2 cannot be directly applied to this model. Therefore, the values relevant to F_1 and F_2 have been normalized.

With an equation linking melt fraction and temperature having been derived, an equation linking da/dt, the variation in melt layer radius over time, and dT_L/dt, the variation of the thermal evolution of a melt layer over time, was needed for comparison to the model formulated based on Labrosse et al. By finding the derivative of Eq. 9:

$$\frac{\mathrm{d}F}{\mathrm{dt}} = \frac{3a^2}{a_0^3 - b^3}\frac{\mathrm{d}a}{\mathrm{dt}} \qquad \text{Eq. 11,}$$

a new equation could be derived, linking the two parameters. This equation was:

$$\frac{\mathrm{d}a}{\mathrm{dt}} = \frac{a_0^3 - b^3}{3a^2}\frac{\mathrm{d}F}{\mathrm{dT_L}}\frac{\mathrm{d}T_L}{\mathrm{dt}} \qquad \text{Eq. 12.}$$

Thermal history and evolving melt layer thickness have been solved for in conjunction with Eq. 5. Nondimensionalization was again required to solve the system of equations. The nondimensionalized version of Eq. 12 is as follows:

$$\frac{\mathrm{d}a}{\mathrm{dt}} = \frac{1-\left(b/a_0\right)^3}{3a^2}\frac{\mathrm{d}F}{\mathrm{dT_L}}\frac{\mathrm{d}T_L}{\mathrm{dt}} \qquad \text{Eq. 13.}$$

Thermal Evolution of the Mantle

Based on the Simplified Thermal History Model, a new equation has been included to incorporate the effects of an evolving mantle temperature on the thermal evolution and internal structural evolution of the magma ocean. An equation for mantle thermal evolution was derived from the heat equation, as in the case of the simplified model. The equation incorporates radiogenic heating and heat flux through the mantle, including a term for convective heat loss within the mantle.

$$\frac{dT_m}{dt} = \left(\frac{1}{M_m C_{pm}}\right)\left[He^{-\lambda t} - 4\pi R_m^2 k \frac{\left(T_m - T_s\right)^{\beta+1}}{R_m - a}\left(\frac{\alpha g}{\kappa \upsilon_0}\frac{\left(R_m - a\right)^3}{Ra_{cr}}\right)^{\beta} e^{\frac{-\beta A_0}{T_m}}\right] \qquad \text{Eq. 14}$$

Results

Simplified Thermal History Model

Figure 5 illustrates both the thermal history of the Earth and the variation of viscosity within the mantle over time, as determined from a reproduced version of the simplified thermal evolution model originally produced by Schubert et al. One can observe from these plots that the initial temperature of the mantle, after accretion of the Earth, is a large value, while the corresponding initial viscosity is a small value. Temperature then undergoes a rapid decline as the Earth convects vigorously to get rid of excess heat. Conversely, the viscosity undergoes a rapid increase. As temperature begins to decrease, viscosity is increasing due to crystallization within the magma ocean. The viscosity increases several orders of magnitude, which is what is expected as the rheological transition within the magma ocean propagates towards the surface (Solomatov, 2000). If a global magma ocean was formed early in Earth's history, this is what one would expect to see. These rapid changes extend over a period of 200-300 Myr, according to this model. After this stage, the mantle undergoes a more gradual cooling, as suggested by the much shallower decline in temperature present on the plot in Figure 5.

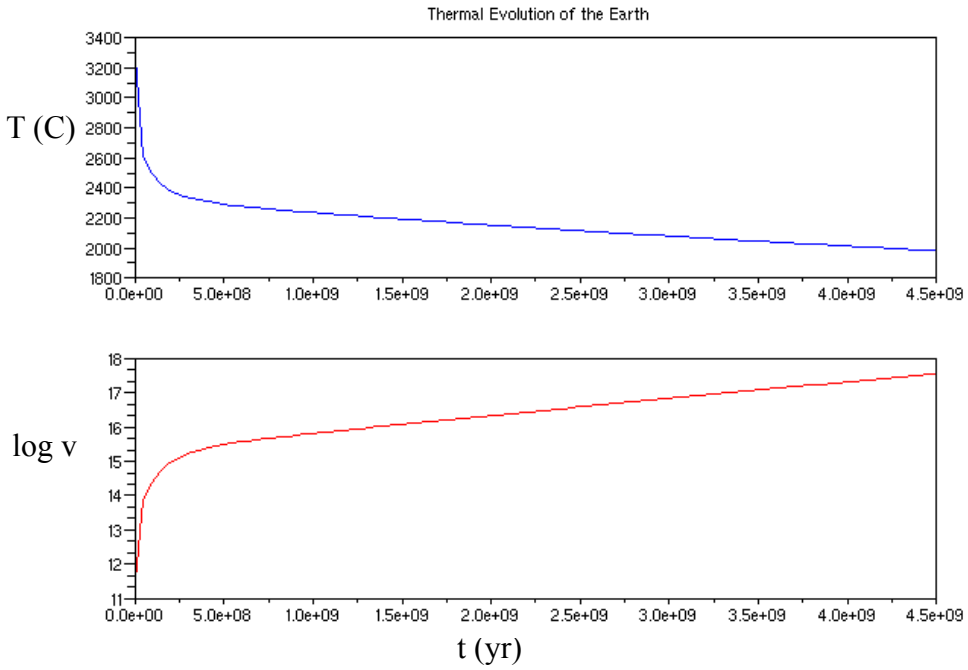

Figure 5: STHM Results - This is the reproduced thermal evolution model from Schubert et al. The top plot is depicting the temperature variation over time, from 4.5 Gyr to present. The bottom plot is depicting the viscosity variation of the mantle over time.

Thermal Evolution and Melt Layer Evolution: Linear v. Nonlinear Crystallization Models

The plots of thermal evolution and thickness evolution created from Equations 5-8 are not exactly the same as the plots originally produced by Labrosse et al. Overall, the general trends are the same, but not exact. The values used in my equations are the same as those used by Labrosse et al., with the exception of the radiogenic heating term. Though Eq. 5 expresses radiogenic heating as a function of time (H(t)), Labrosse et al. do not clearly indicate an expression for H(t). Thus, the H value used for this model was determined by other means, and is likely different from the value used by Labrosse et al. It is possible that the H value used for these plots contributed to the variation. Figure 6 is a plot illustrating the difference between two reproduced thermal evolution models: one depicting thermal evolution when H is equivalent to 0, and one depicting thermal evolution calculated with a predetermined H value. As you can see from the plot, the radiogenic heating does influence thermal evolution.

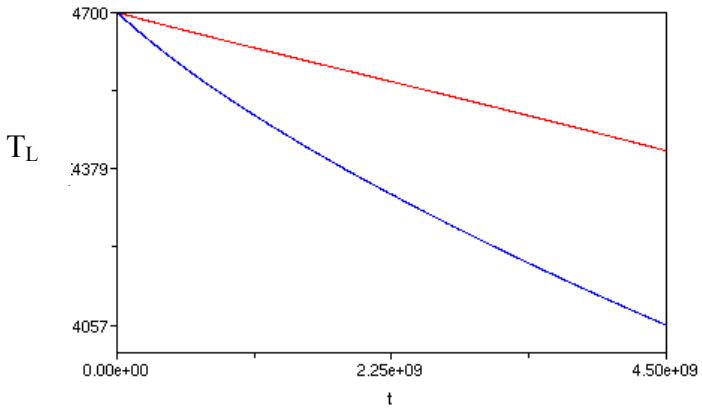

Figure 6: Radiogenic Heating Plot - This figure is plotting the thermal evolution (T_L v. t (yr)) of the mantle without contribution from radiogenic heating (blue) and thermal evolution of the mantle with radiogenic heating (red).

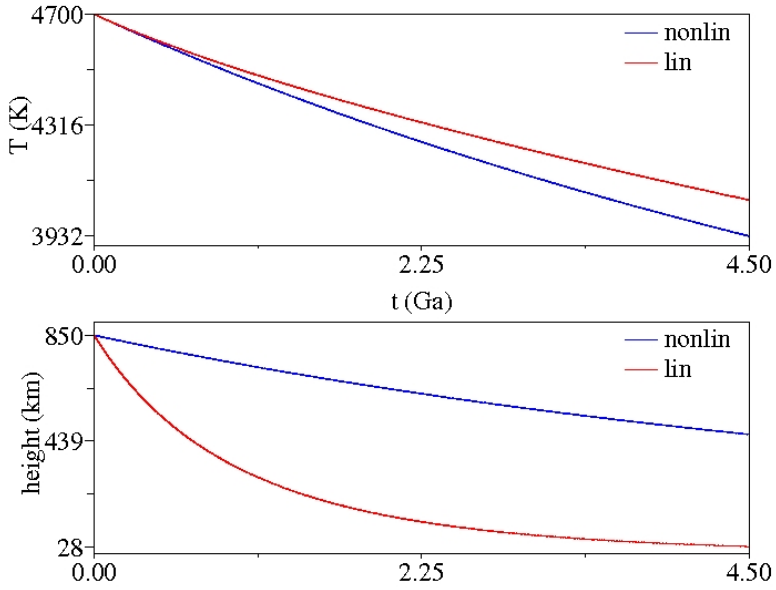

Figure 7: Comparing Thermal Evolution Models - The top figure is comparing the thermal evolution models (Temperature TL v. Time t (Gyr) derived from the linear crystallization model (red) and nonlinear crystallization model (blue). The bottom figure is comparing the thickness evolution (Upper melt layer radius a v. Time t) derived from both the linear and nonlinear crystallization models as well.

A comparison of the two thermal evolution models and melt layer thickness evolution models derived from both linear and nonlinear crystallization models can be seen in Figure 7. Of the two cooling trends, the model derived from the nonlinear crystallization equations shows a greater decline in temperature, and thus predicts a lower present day melt layer temperature. Conversely, the nonlinear melt layer thickness model shows a much smaller decline in thickness when compared with the linear model. The linear model predicts a present day melt layer thickness approximately ¼ of its original value for the given parameters, while the nonlinear model predicts a much smaller decrease in thickness. These results would imply that a substantial magma ocean should still exist today.

The maximum error determined from the results of the thermal evolution models is approximately 6E-8 K. This was determined by taking 10^3 data points over a nondimensionalized temperature interval spanning 0.2. Thus, the average step size is calculated to be approximately 2E-4. The maximum error is minimal when compared with the calculated temperature values.

Thermal Evolution of the Mantle

Trends for both the thermal and internal structural evolution of a magma ocean incorporating an evolving mantle temperature are similar to those using a constant mantle temperature. However, the magnitude of change has a more pronounced variation. The results incorporating the mantle temperature evolution predict a much lower present day magma ocean temperature for both the linear and nonlinear model. Likewise, these results also predict a more depleted magma ocean thickness. Figure 8 depicts the results for both the thermal and thickness evolution after incorporating an evolving mantle temperature. It also includes a plot of the thermal evolution of the mantle which is the same for both the linear and nonlinear model, as it should be.

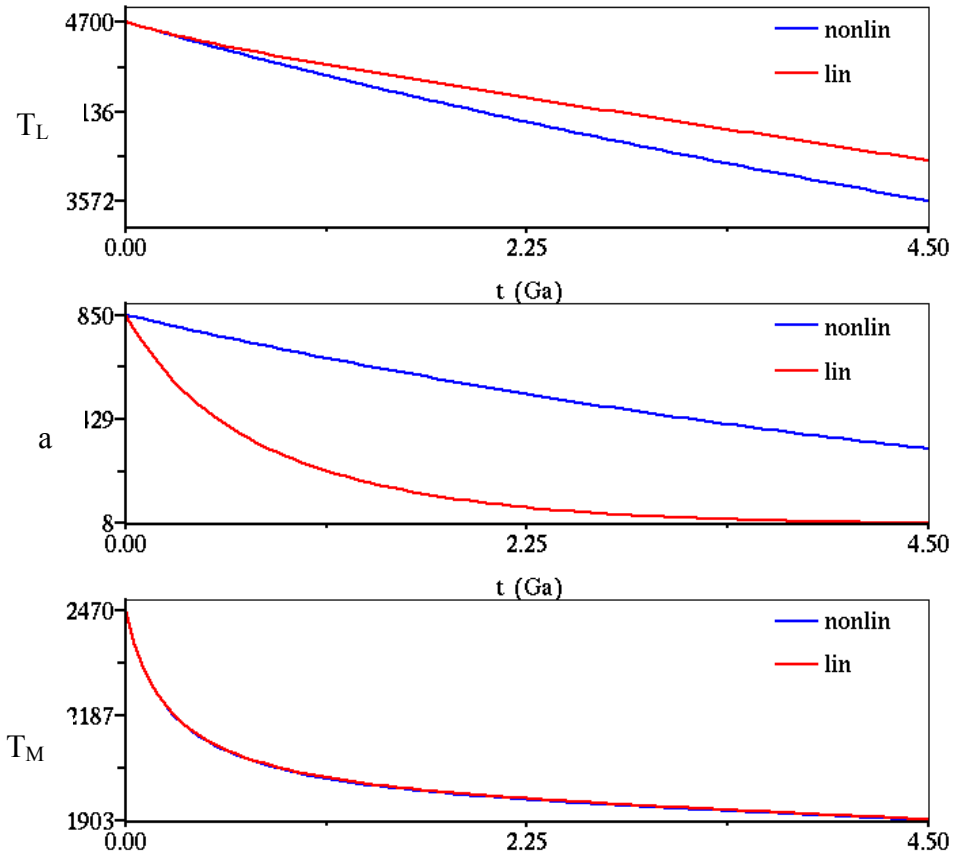

Figure 8: Thermal Evolution and Mantle Evolution - These results incorporate an evolving mantle temperature's influence on magma ocean evolution. The top most plot shows thermal evolution of the melt layer. The middle plot depicts thickness evolution. The bottom plot depicts thermal evolution of the mantle.

Discussion

The results of this study show that, as expected, there is variation in the evolutionary trends determined using linear and nonlinear mantle crystallization models. This emphasizes the necessity of using a more realistic crystallization model, when possible, to determine thermal evolution within a planetary body. Considering this, it is important to note that the nonlinear crystallization model used here, while more realistic than a linear crystallization model, must still be improved upon.

The crystallization model from Katz et al. was originally derived for upper mantle melting and crystallization. The model derived here, based on the research from Katz et al., was normalized to be used for magma ocean conditions. Thus, there are two problems with this model. Petrologic data is limited for the lowest portions of the mantle and core-mantle boundary. Without more accurate data, it is difficult to constrain a better crystallization model.

A second problem has to do with the liquidus temperature used to determine the thermal evolution of the magma ocean. The way the model has been derived, it is impossible to reach temperatures above the liquidus temperature. This is also unrealistic as temperatures should be

able to increase beyond the liquidus temperature given enough heating. This is an issue that may be addressed by incorporating a different crystallization model.

2. Triton's Subsurface Cryomagma Ocean

Introduction

The icy satellite Triton, currently orbiting Neptune, has been of great interest to the scientific community because of its geologic surface features, similar to those on Europa, as well as its characteristic orbital parameters. As the schematic diagram in Figure 9 displays, Triton is believed to contain a large silicate core; overlain by a cryomagma ocean; which in turn, is enclosed by an ice shell predominantly composed of H_2O, but containing trace amounts of ammonia and other volatile elements (Hussmann et al., 2006). Marring the surface of the planet, which is relatively young, are a series of ridges similar to those found on Europa. It has been suggested that the appearance of these unique ridges may have indirectly resulted from Triton's orbital evolution (Prockter et al., 2005).

Recent studies estimate Triton's surface age to be within 10 and 100 Myr based on the density of impact craters found on the satellite's surface (Schenk and Zahnle, 2007). Though there is some variation within this estimate depending on the type of impact, researchers believe the estimate should be more recent, closer to 10 Myr. Though the age of the ridges found on Triton have not been approximated, it is likely they have formed relatively recently (Prockter et al., 2005). In addition to these ridges, researchers have also observed other features such as possible geyser and plume activity and volcanic plains, as evidence of geologic activity occurring some time in Triton's past (Brown and Kirk, 1994; Schenk and Zahnle, 2007). Though several hypotheses have been put forth to explain these occurrences, one possible hypothesis suggests that the satellite may still be active at present. If the satellite is still active, what is driving and sustaining this geologic activity?

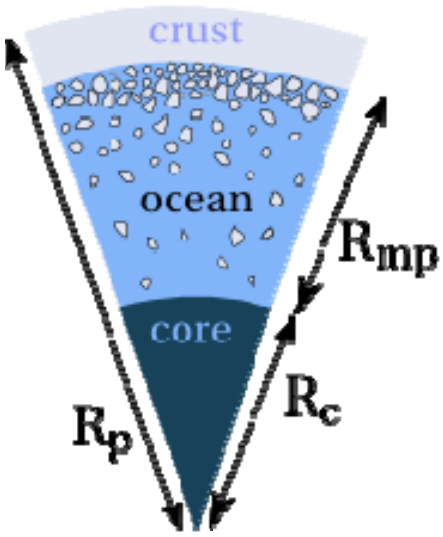

Figure 9: Triton's Interior - This diagram illustrates the internal stratification of Triton.

Triton, at present, has an inclined and circular retrograde orbit (Ross and Schubert, 1990). Its distinct orbital parameters have led researchers to question how Triton came to orbit Neptune. It is now believed that Triton originally had a heliocentric orbit, but was later caught in orbit around Neptune. One hypothesis is that the satellite was captured in a binary-planet exchange (Agnor and Hamilton, 2006). Another hypothesis suggests that the satellite may have been captured during a close encounter with Neptune, or a series of close encounters, causing a dissipation of orbital energy via gas drag (McKinnon and Leith, 1995). Triton's original heliocentric orbit and post-capture orbit would have been much more elliptical when compared to its current orbit. Thus, sometime after Triton's capture, the satellite's orbit began to circularize. An earlier study by Ross and Schubert (1990) models the coupling of Triton's dynamical evolution with the thermal evolution of the satellite from tidal heating alone. From this model, they deduced that the circularization of Triton's orbit may have occurred abruptly in one event. The circularization of the orbit would have contributed to excessive heating within the planet's interior from the resulting tidal dissipation. The amount of heating from tidal dissipation would have been significant enough to create a subsurface cryomagma ocean (Ross and Schubert, 1990).

Prockter et al. suggested that the ridges found on Triton's surface may have resulted from tidal stresses, caused by Triton's orbit, relatively recently based on the estimated surface age of the satellite (2005). Triton's current orbit, however, is circular. This would imply that the orbit had to have undergone recent circularization. This assumption, though, is contrary to the binary-planet exchange capture hypothesis, which suggests that the satellite was more likely captured early in the solar system's history, when more Triton-like bodies were prevalent (Agnor and Hamilton, 2006).

An alternative hypothesis is that the geological activity may be a result of internal processes and heating. Tidal dissipation from a circularizing orbit would have contributed to the internal heating necessary to sustain geologic activity. Such a scenario could be more appropriate for a capture scenario occurring earlier in the solar system's evolution. The heating of the interior would then suggest the existence of a subsurface magma ocean. For this reason, it is necessary to explore whether a magma ocean does exist within Triton's interior. If such an ocean does exist, what is its extent within the satellite's interior, and under what conditions has it been maintained?

Objectives

Heat remaining within the satellite's interior may be responsible for the unique geological activity seen on Triton's surface. Some researchers have suggested that the surface geological features may have been formed from diurnal stresses caused by Triton's orbital eccentricity (Prockter et al., 2005). As Triton's orbit is currently circular, however, diurnal stresses would not be great enough to explain these features, assuming they have been created relatively recently. Heat remnant from tidal heating contributions during the circularization process may provide an alternative explanation. By analyzing the thermal evolution of the satellite, we may determine whether a significant source of heat is currently present and capable of contributing to these features. We may also determine whether a subsurface cryomagma ocean exists within Triton's interior and its extent at present. My hypothesis is that a cryomagma ocean does still exist within the satellite's interior. Within the study, we will begin to explore the possible existence of a subsurface ocean within Triton's interior.

Experiment Design

To ultimately determine the existence of a subsurface ocean, this study first explores the thermal structure of Triton's interior. For simplicity, this study subcategorizes Triton's interior into three layers: an ice I shell crust, a multiphase layer, and a silicate core. As stated previously, Triton's outer layer is mostly composed of H_2O. The divariant, multiphase layer consists of an H_2O ice and an $NH_3 - H_2O$ liquid for a 10% NH_3 composition.

Composition of the Crust

Triton's crust is essentially composed entirely of H_2O ice I, which is a low pressure form of ice. For this composition, the shell should thermally evolve according to the phase diagram in Figure 10. For simplicity, we could assume an entirely pure H_2O composition for the entire satellite. This would imply a pure H_2O solid crust, and a pure H_2O multiphase layer. Such a scenario would provide a simple starting point for determining the thermal structure within Triton's interior as ammonia represents a small percentage of the overall composition. However, the results of such a model would be unrealistic. Based on the phase diagram, temperature should decrease, as pressure increases. Thus, the temperature within the satellite should decrease below the surface temperature of the satellite as depth increases. Even incorporating a tidal

heating of approximately 2 GW, based on Ross and Schubert's earlier study of Triton's evolution, it would be difficult to maintain a pure H_2O ocean at present. This demonstrates the necessity of incorporating minor additional compositions in the model. In this case, the presence of ammonia cannot be ignored. Incorporating ammonia provides the only method of obtaining a subsurface ocean at present.

NH_3 and H_2O Mixture Model

For this mixed composition model, incorporating 10% NH_3, the surface temperature of the crust (T_{surf}) has been preset to 38K, as estimated by the Voyager mission (Brown and Kirk, 1994). A crustal thickness of 15 km has also been prescribed (Ruiz, 2003). In this model, the temperature profiles of both layers have been derived from the heat equation as well. The multiphase layer no longer follows the clapeyron slope. Instead, we rely on the phase diagram in Figure 11 to determine crystallization within the multiphase layer. Based on the concentration of ammonia, new boundary conditions have been set for the multiphase layer. The temperature at the boundary between the crust and the multiphase layer is 176K, which is the solidus for the ammonia and H_2O mixture. The base of the multiphase layer is 240K, which is the liquidus for the ammonia and H_2O mixture. Although these conditions are not ideal for this system, they present a simpler scenario to build upon.

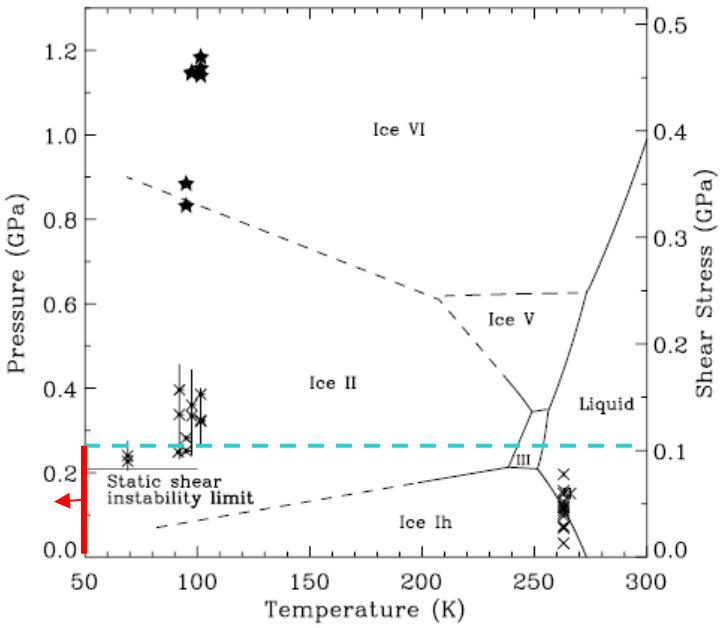

Figure 10: Ice I Phase Diagram - This is an H_2O phase diagram borrowed from Stewart and Ahrens, 2005. Triton's composition falls within the Ice Ih range. The blue dotted line marks the Core-Mantle Boundary, which occurs at a radius of approximately 1017 km. The red line and arrow has been shown to note that the surface temperature of Triton, 38 K, is cooler than the lower limit of this plot.

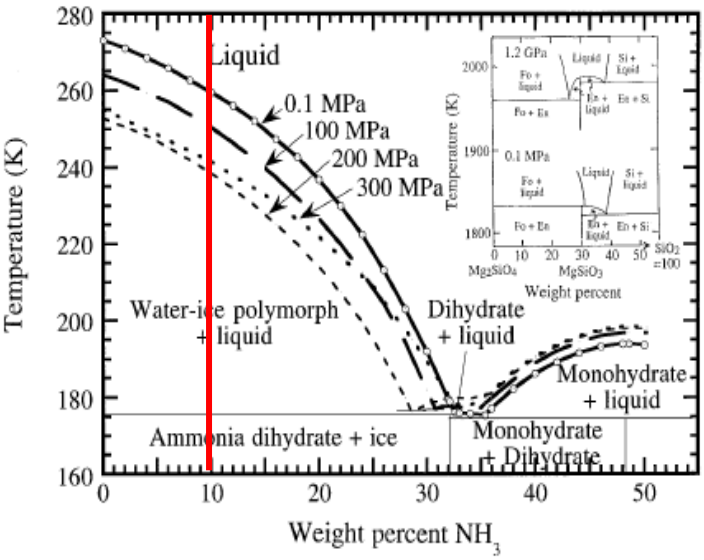

Figure 11: NH_3 – H_2O Phase Diagram – Diagram borrowed from Hogenboom et al., 1997. The red line represents the concentration of ammonia used within our model.

Governing Equations

NH_3 and H_2O Mixture Model

The boundary conditions for the crust include:

At the surface:	z = 0	$T = T_{surf}$
At the base:	z=h	$T=T_s$

From the heat equation, the temperature of the crust can be found as a solution to

$$\rho c_p \frac{\mathrm{D}T_c}{\mathrm{Dt}} = k\nabla^2 T_c + \rho\Psi \qquad \text{Eq. 15,}$$

where ρ is density, cp is specific heat, k is thermal conductivity, and Ψ is tidal dissipation.

$$\frac{\mathrm{D}T}{\mathrm{Dt}} = \frac{\partial T}{\partial t} + v\frac{\partial T}{\partial z} \qquad \text{Eq. 16}$$

For this simplified model of Triton, however, we assumed steady state conditions to derive equations necessary to describe the temperature within each of Triton's layers. Thus, we set $\frac{\mathrm{D}T}{\mathrm{Dt}} = 0$ in the crust as the system is not changing in time or varying spatially. We then find Eq. 15 to become

$$k\frac{\partial^2 T_c}{\partial z^2} = -\rho\Psi \qquad \text{Eq. 17.}$$

The boundary conditions for the multiphase layer include:

At the surface:	z = h	$T = T_s$
At the base:	$z = R_c$	$T = T_l$

The temperature within the multiphase layer can be found as a solution to

$$\frac{\mathrm{D}T_m}{\mathrm{Dt}} - \frac{T_m \Delta S}{c_p}\frac{\mathrm{D}F}{\mathrm{Dt}} = \frac{k}{\rho c_p}\nabla^2 T_m \qquad \text{Eq. 18,}$$

where ΔS is entropy and F is melt fraction. Crystallization within this layer is defined by

$$F = \left(\frac{T_m - T_s}{T_l - T_s}\right)^{\beta} \qquad \text{Eq. 19,}$$

where β is equal to 1 for a linear model. For this model, tidal heating has been prescribed a constant value. Taking steady state conditions into consideration, we again find that the system will not be varying temporally, only spatially as percolation occurs. Therefore,

$$\frac{\mathrm{D}T_m}{\mathrm{Dt}} = v\frac{\partial T_m}{\partial z}$$

$$\frac{\mathrm{D}F}{\mathrm{Dt}} = v\frac{\partial F}{\partial z} = v\frac{\mathrm{d}F}{\mathrm{dT}}\frac{\mathrm{d}T}{\mathrm{dz}}$$

Equation 18 becomes

$$\left(1 - \frac{T_m \Delta S}{c_p \Delta T}\right) v\frac{\mathrm{d}T_m}{\mathrm{dz}} = \frac{k}{\rho c_p}\frac{\mathrm{d}^2 T_m}{\mathrm{dz}^2} \qquad \text{Eq. 20,}$$

where z is depth.

Results

NH_3 and H_2O Mixture Model

After analyzing equations 19 and 20, the geothermal gradient for an ammonia and H_2O mix can be determined by:
Temperature of the crust:

$$T_c = T_{surf}\left(1-\frac{z}{h}\right)+T_s\frac{z}{h}+\rho\Psi z\frac{(h-z)}{2k} \qquad \text{Eq. 21,}$$

where T_s is the solidus temperature, z is depth beneath the satellite's surface, and h is ice shell thickness.
Temperature of the multiphase layer:

$$T_m = \frac{\alpha(T_l-T_s)}{e^{\alpha(R-r_c)}-e^{\alpha h}}\frac{e^{\alpha z}}{\alpha}+\frac{1}{\alpha}\left(T_s\alpha-\frac{\alpha(T_l-T_s)}{e^{\alpha(R-r_c)}-e^{\alpha h}}e^{\alpha h}\right) \qquad \text{Eq.22,}$$

where

$$\alpha = \rho c_p\frac{v}{k}\left(1-\frac{\Delta H}{\Delta T c_p}\right) \qquad \text{Eq. 23.}$$

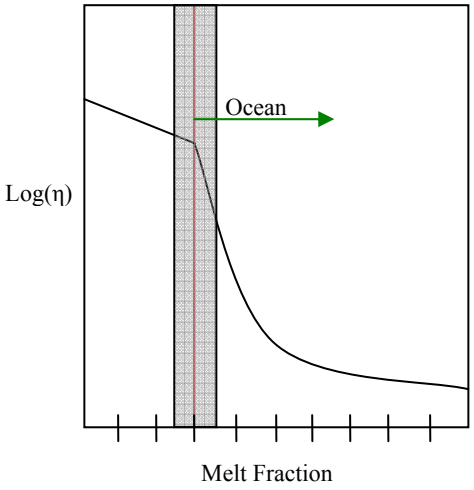

Figure 12: Viscosity v. F - Sketch of relationship between viscosity and melt fraction. For a melt fraction greater than approximately 0.3, a magma ocean is possible.

T_l is the liquidus temperature, ΔH is enthalpy, ΔT is the difference between the liquidus and the solidus, and v is the segregation velocity between crystal and melt. The segregation velocity within this layer occurs as a result of density driven percolation of the heavy fluid through the crystal matrix. It is defined as

$$v = \frac{k}{\mu}\Delta\rho g \qquad \text{Eq. 24,}$$

which is a simplified form of Darcy's law. The viscosity μ is assumed to be ~10^{-3} Pa s. The change in density is between 996 and 916 kg m^{-3}. The calculated value for g is approximately .78 ms^{-2}. For comparison, three values of k were used, corresponding to three values for segregation velocity. The k values included 8 x 10^{-9}, 5 x 10^{-10}, 8 x 10^{-12}.

The results of the second model, incorporating ammonia are illustrated in Figure 13. Figure 12 represents how viscosity evolves with increasing melt fraction. A high viscosity is maintained for a low melt fraction. However, melt fractions greater than ~0.3, the critical rheological melt fraction, allow for the existence of a subsurface ocean. The 0.3 melt fraction boundary is marked by an abrupt decrease in melt

viscosity. This transition occurs as the crystal faces lose interaction. This boundary has been marked in Figure 13 for discussion.

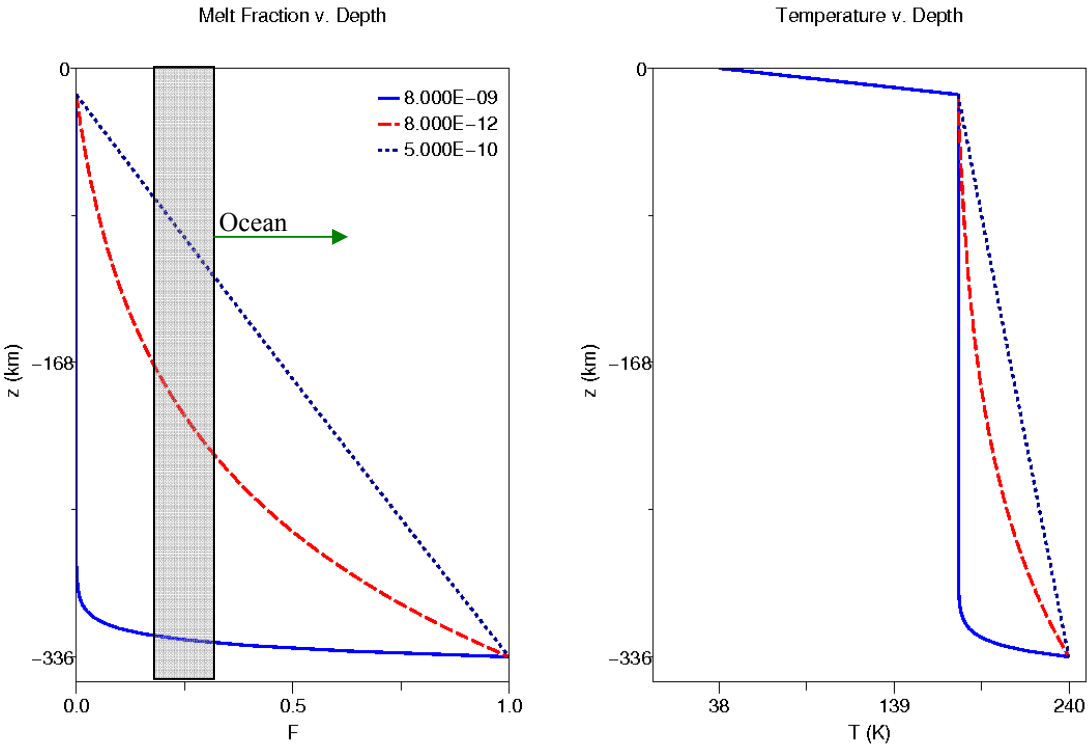

Figure 13: Triton's Temperature Profile - Plot of Melt Fraction and Temperature v. Depth for a composition of ammonia and water ice. The shaded grey box represents the range for a critical rheological melt fraction. As the green arrow indicates, melt fractions larger than this value may constitute a cryomagma ocean.

Crystallization within this layer is based on the phase diagram in Figure 11. This model has been analyzed for three different segregation velocities within the multiphase layer. The model for the fastest velocity undergoes little change in melt fraction or temperature until the very base of the multiphase layer, where both of these values experience a sharp increase. Conversely, the model for the slowest velocity experiences a more gradual increase in both temperature and melt fraction until the liquidus has been reached at the base of the layer.

Discussion

The results of the first part of this study suggest the existence of a remnant basal magma ocean within the Earth's interior at present. Ultimately, after completing the analysis of Triton's evolution, it will also become apparent whether or not a cryomagma ocean exists today to help explain the icy satellite's geologic features. The current results obtained from the simpler Triton models are not yet adequate for successfully determining whether or not a cryomagma ocean exists within the satellite's interior. Rather these models discern the thermal structure of Triton's interior. They also illuminate several problems that must be addressed before an accurate model can be attained.

First, the models shown here illustrate the necessity of incorporating ammonia within the

satellite's composition. The presence of ammonia greatly reduces the liquidus and solidus temperatures within the crust and multiphase layer. Therefore, the dominance of crystals versus melt within the multiphase layer will be greatly influenced as well. Incorporating ammonia increases the likeliness of sustaining a cryomagma ocean at present. Even though ammonia constitutes a small portion of the ice composition, it should be included within the final model for the most accurate results.

The results from the model incorporating ammonia also demonstrate the influence of the segregation velocity within the multiphase layer. A larger segregation velocity encourages a predominantly crystallized multiphase layer. At the base of this layer, however, a sharp increase in melt fraction and temperature may suggest the existence of a basal cryomagma ocean with a higher melt fraction, formed after most of the melt has percolated through the crystallized phase. Conversely, a slower segregation velocity encourages much more gradual increases in melt fraction and temperature. Based on Figure 14, we see that a significant magma ocean does exist, amounting to more than half of the multiphase layer in this case. This magma ocean, however, contains a larger fraction of crystals than in the higher velocity case, and is, therefore, more thoroughly mixed. This plot illustrates that a magma ocean may exist within Triton's interior, based on the prescribed conditions, but its extent within the satellite's interior will vary with the melt segregation velocity.

A third problem with this model is the assumptions made by the boundary conditions. For example, within the NH_3 and H_2O model, the temperature at the base of the multiphase layer was prescribed at 240K, the liquidus temperature. This ultimately forces the system to eventually obtain a melt fraction of 1 at the base of the multiphase layer. In future models coupling orbital and thermal evolution, this restriction can not be imposed as it eliminates the option of obtaining a completely crystallized subsurface ocean. Another restriction was prescribing a set crustal thickness. This, however, will be eliminated by evolving this model to a moving boundary problem. For this study, these conditions were set for simplification. Thus, the next models will not rely on these conditions.

The Triton models shown here do not show the thermal evolution of the satellite since it's capture, but a snapshot of the satellite's geothermal gradient and internal structure. The largest heat contributions within the satellite would ordinarily be radiogenic heating and tidal heating. However, the radiogenic heating within the satellite's core is negligible compared to the tidal heating contributed by the satellite's orbital evolution. Therefore, radiogenic heating has not been included in discerning temperature within Triton's interior. The tidal heating is thus the main source of heating within these equations.

Because tidal heating is so prevalent within the thermal evolution of the satellite, it is important to obtain an accurate model for the orbital evolution of the satellite, which will allow for a more accurate determination of the tidal heating parameter Ψ. Within these solutions, Ψ has not been derived based on orbital evolution. By incorporating orbital evolution of the satellite from its time of capture to the circularization of its orbit, we should see the interior respond more appropriately to tidal heating, possibly allowing for the existence of a subsurface ocean.

Future Work

This study has only begun to explore one element of the question regarding the existence of a magma ocean at present. The next step will be to determine the thermal evolution of the satellite coupled with Triton's orbital evolution since capture. To ultimately determine the thermal evolution of Triton's interior, this study will eventually analyze the evolution of three

distinct layers: the crust, the mush layer, and the cryomagma ocean. Thus, the model will numerically analyze for three evolving temperatures: crust temperature, T_c; mush layer temperature, T_m; and ocean temperature, T_o. As temperature decreases and crystallization occurs, the thickness of both the cryomagma ocean and the mush layer will evolve. Therefore, this problem will become a moving boundary problem with evolving mush layer radius, r_m, and ocean radius, r_o.

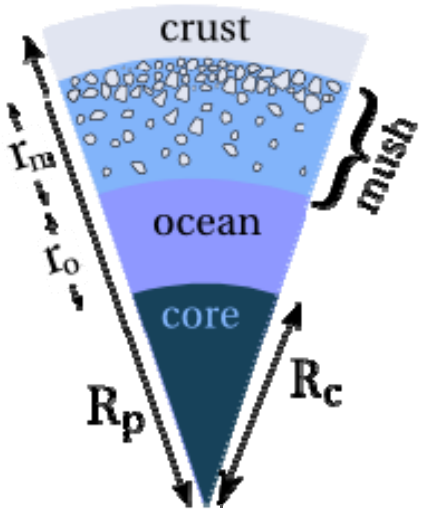

Figure 14: **Triton's Interior 2** - This diagram illustrates the internal stratification of Triton.

The final model will determine thermal evolution by solving for three equations derived from the heat equation, representing thermal evolution within each layer of the satellite. These equations include the following:

Equation for thermal evolution of the crust:

$$\rho c \frac{\partial T_c}{\partial t} = -\nabla \cdot q_c + \alpha_c \psi \qquad \text{Eq. 25}$$

Equation for thermal evolution of the mush layer:

$$\rho c \left(\frac{\partial T_m}{\partial t} + u_m \cdot \nabla T_m \right) = -\nabla \cdot q_m + \alpha_m \psi + L \qquad \text{Eq. 26}$$

$$L = \rho T_m \Delta s \left(\frac{\partial F}{\partial t} + u_m \cdot \nabla F \right)$$

Equation for thermal evolution of the cryomagma ocean:

$$\rho c \left(\frac{\partial T_o}{\partial t} + u_o \cdot \nabla T_o \right) = -\nabla \cdot q_o + \alpha_o \psi \qquad \text{Eq. 27}$$

Ψ represents tidal heating within each layer of the satellite. As it is unclear how tidal heating may distribute within the satellite's interior, an α coefficient has been introduced to control tidal heating distribution. The sum of the three α's will be 1. An additional two terms unique to these equations include the u_m and u_o terms. u_m represents the percolation or segregation velocity of the crystallizing mush layer, which serves as a means of heat transfer within that layer. u_o represents the turbulent velocity within the cryomagma ocean, which affects heat transfer throughout the ocean. Using these equations, we will numerically solve for Triton's thermal evolution to determine a subsurface ocean's existence.

3. Conclusion

Magma oceans may be found in various forms throughout the solar system, but can exhibit similar dynamics while evolving within a planetary body. By modeling their evolution, one can gain a more thorough understanding of how the planetary body has evolved to its current state and what effect the presence of a magma ocean has had on both the internal and external features of the planet. Thus, modeling a magma ocean's thermal evolution as accurately as possible can provide information on processes and features affected by its presence, such as the geological surface features of Triton mentioned previously. Furthermore, it is always necessary to continuously improve methods of modeling a magma ocean's evolution to achieve the most accurate thermal history, as it largely impacts the planetary bodies history, as well.

This study has explored the evolution of a terrestrial basal magma ocean using a nonlinear crystallization model as an alternative to previous studies, which have relied on linearized models. The study has shown that a nonlinear model provides a significantly different thermal history when compared with that of the linearized model. This illustrates the preference for a more realistic nonlinearized crystallization model, when analyzing thermal and structural evolution, for attaining a more accurate evolution of a magma ocean.

This study has also begun to explore the effects of crystallization on Triton's subsurface cryomagma ocean. Here, we have explored the thermal structure of Triton to see if a subsurface ocean could potentially exist at present. Our results have shown that a subsurface ocean is possible given certain conditions, but these results are not a reflection of the satellite's evolution. This study will be continued to determine whether or not a cryomagma ocean does exist at present and how it has evolved from its initial formation.

4. Acknowledgements

I would like to thank Dr. Saswata Hier-Majumder for his guidance, support, and endless patience throughout the duration of this research. I would also like to thank Dr. Laurent Montesi for his thoughtful advice and suggestions regarding the modeling in this project. Finally, a special thanks to the Geodynamics Reading Group for their helpful suggestions.

5. References

[1] Abe, Yutaka. "Thermal and chemical evolution of the terrestrial magma ocean." Physics of the Earth and Planetary Interiors 100 (1997): 27-39.

[2] Agnor, Craig B., and Douglas P. Hamilton. "Neptune's capture of its moon Triton in a binary-planet gravitational encounter." Nature 441 (2006): 192-94.

[3] Brown, Robert H., and Randolph L. Kirk. "Coupling of volatile transport and internal heat flow on Triton." Journal of Geophysical Research 99 (1994): 1965-981.

[4] Durham, W. B., and L. A. Stern. "Rheological properties of Water Ice-Applications to Satellites of the Outer Planets." Annu. Rev. Earth Planet. Sci. (2001): 295-326.

[5] Elkins-Tanton, L. T. "Linked magma ocean solidification and atmospheric growth for Earth and Mars." Earth and Planetary Science Letters 271 (2008): 181-91.

[6] Feistel, Rainer, and Wolfgang Wagner. "A New Equation of State for H2O Ice Ih." Journal of Physical and Chemical Reference Data 35 (2006): 1021-047.

[7] Goldreich, P., N. Murray, P. Y. Longaretti, and D. Banfield. "Neptune's Story." Science 245 (1989): 500-04.

[8] Hogenboom, D. L., J. S. Kargel, G. J. Consolmagno, T. C. Holden, L. Lee, and M. Buyyounouski. "The Ammonia-Water System and the Chemical Differentiation of Icy Satellites." Icarus 128 (1997): 171-80.

[9] Hussmann, Hauke, Frank Sohl, and Tilman Spohn. "Subsurface oceans and deep interiors of medium-sized outer planet satellites and large trans-neptunian objects." Icarus 185 (2006): 258-73.

[10] Hustoft, Justin, Ted Scott, and David L. Kohlstedt. "Effect of metallic melt on the viscosity of peridotite." Earth and Planetary Science Letters 260 (2007): 355-60.

[11] Katz, Richard F., Marc Spiegelman, and Charles H. Langmuir. "A new parameterization." Geochemistry Geophysics Geosystems 4 (2003).

[12] Labrosse, S., and C. Jaupart. "Thermal Evolution of the Earth: Secular changes and fluctuations of plate characteristics." Earth and Planetary Science Letters 260 (2007): 465-81.

[13] Labrosse, S., J. W. Hernlund, and N. Coltice. "A crystallizing dense magma ocean at the base of the Earth's mantle." Nature 450 (2007): 866-69.

[14] Leliwa-Kopystynski, Jacek, Minoru Maruyama, and Toshiu Nakajima. "The Water-Ammonia Phase Diagram up to 300 MPa: Application to icy Satellites." Icarus 159 (2002): 518-28.

[15] McKinnon, William B. "On convection in ice I shells of outer Solar System bodies, with detailed application to Callisto." Icarus 183 (2006): 435-50.

[16] McKinnon, William B., and Andrew C. Leith. "Gas Drag and the Orbital Evolution of a Captured Triton." Icarus 118 (1995): 392-413.

[17] Peale, S. J. "Origin and Evolution of the Natural Satellites." Annu. Rev. of Astron. Astrophys. 37 (1999): 533-602.

[18] Press, William H., Saul A. Teukolsky, and William T. Vetterling. Numerical Recipes in FORTRAN 77 Vol. 1 : The Art of Scientific Computing. 2nd ed. Vol. 1. New York: Cambridge UP, 1992. 704-16.

[19] Prockter, Louise M., Francis Nimmo, and Robert T. Pappalardo. "A Shear Heating Origin For Ridges on Triton." Geophysical Research Letters 32 (2005).

[20] Ross, Martin N., and Gerald Schubert. "The Coupled Orbital and Thermal Evolution of Triton." Geophysical Research Letters 17 (1990): 1749-752.

[21] Rubie, D. C., H. J. Melosh, J. E. Reid, C. Liebske, and K. Righter. "Mechanisms of metal-silicate equilibration in the terrestrial magma ocean." Earth and Planetary Science Letters 205 (2003): 239-55.

[22] Ruiz, Javier. "Heat flow and depth to a possible internal ocean on Triton." Icarus 166 (2003): 436-39.

[23] Schenk, Paul M., and Kevin Zahnle. "On the negligible surface age of Triton." Icarus 192 (2007): 135-49.

[24] Schubert, Gerald, Donald L. Turcotte, and Peter Olson. "Thermal History of the Earth." Mantle Convection in the Earth and Planets Part 2. New York: Cambridge UP, 2001. 586-632.

[25] Scott, T., and D. L. Kohlstedt. "The effect of large melt fraction on the deformation behavior of peridotite." Earth and Planetary Science Letters 246 (2006): 177-87.

[26] Solomatov, V. S. "Fluid Dynamics of a Terrestrial Magma Ocean." Origin of the Earth and Moon. By Robin M. Canup and Kevin Righter. New York, AZ: University of Arizona P, 2000. 323-38.

[27] Solomatov, Viatcheslav S., and David J. Stevenson. "Nonfractional Crystallization of a Terrestrial Magma Ocean." Journal of Geophysical Research 98 (1993a): 5391-406.

[28] Solomatov, Viatcheslav S., and David J. Stevenson. "Suspension in Convective Layers and Style of Differentiation of a Terrestrial Magma Ocean." Journal of Geophysical Research 98 (1993b): 5375-390.

[29] Stewart, Sarah T., and Thomas J. Ahrens. "Shock Properties of H2O ice." Journal of Geophysical Research 110 (2005).

Honor Code

"I pledge on my honor that I have not given or received any unauthorized assistance or plagiarized on this assignment."

_____ _____